Bone Reports 23 (2024) 101815

Contents lists available at ScienceDirect

Bone Reports

journal homepage: www.elsevier.com/locate/bonr

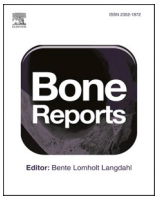

Naringin promotes osteogenic potential in bone marrow-derived mesenchymal stem cells via mediation of miR-26a/Ski axis

Jiawei Zou, Longze Zhou, Guoqiang Liu, Ying Zhang, Lingguo Zeng *

Department of Traumatic Orthopedics, Yuebei People's Hospital Affiliated to Shantou University School of Medicine, Shaoguan 512026, China

ARTICLE INFO

Keywords:
ONFH
Naringin
miR-26a
Ski

ABSTRACT

Background: Osteonecrosis of the femoral head (ONFH) is a common orthopedic disease, which seriously affects the quality of life of patients. Naringin has protective effect on ONFH. In present study, we aimed to investigate the mechanism of Naringin regulating miR-26a in ONFH.

Methods: Two sequencing datasets (GSE89587 for micro-RNA, GSE123568 for mRNA) related to ONFH were obtained from the GEO database for bioinformatics analysis. Bone marrow-derived mesenchymal stem cells (BMSCs) were treated with adipogenic medium (AM) or osteogenic medium (OM), and then treated with 10 μM, 100 μM or 1000 μM Naringin. Gene and protein levels were detected by RT-qPCR and Western blotting. ALP activity and alizarin red staining (ARS) were applied to investigate the osteogenic differentiation of BMSCs. Oil red O staining was performed to test adipogenic differentiation. The content of triglycerides (TG) in BMSCs was detected by TG detection kit. Double luciferase reporter gene measured the interaction between miR-26a and Ski.

Results: Bioinfomatic analyses indicated a significant downregulation of miR-26a and a significant upregulation of Ski in the peripheral blood of patients with ONFH. Naringin significantly promoted the osteogenic differentiation, and increased the ALP activity and ARS. Meanwhile, it decreased the adipogenic differentiation and inhibited TG levels. In addition, miR-26a was downregulated and Ski was increased in AM-treated BMSCs, while miR-26a was upregulated and Ski was decreased in OM-treated BMSCs. Furthermore, miR-26a promoted the osteogenic differentiation and suppressed the adipogenic differentiation in BMSCs. Moreover, Naringin enhanced osteogenic potential in BMSCs was reversed by knockdown of miR-26a or overexpression of Ski.

Conclusion: Naringin could promote osteogenic differentiation of BMSCs via mediation of miR-26a/Ski axis. Thereby, Naringin might be a new agent for ONFH treatment.

1. Introduction

Osteonecrosis of the femoral head (ONFH) is an orthopedic disease caused by femoral collapse due to blood supply interruption (Mao et al., 2020). In addition, ONFH can cause the poor life quality of patients (Huang et al., 2020a). It confirmed that excessive glucocorticoid (GC) treatment was the major risk factor for ONFH progression (Guillemet et al., 2020). A previous study indicated that 51 % patients with ONFH were closely related with glucocorticoid (GC) (Kim et al., 2020). Thus, the side effect of GC is the major cause of ONFH. Nowadays, the main treatment of ONFH is drug and surgery, while the effect remains to be improved. Thereby, exploring new methods for ONFH treatment is urgent. It has been reported that traditional Chinese medicine (TCM) is involved in malnutrition of the muscles and bones (Xu et al., 2019a; Xu et al., 2019b). *Drynaria fortunei* is a treatment which is usually used in TCM, and it is thought to strengthen bones and target the key targets of osteoarthritis (Yang et al., 2014). In addition, *Drynaria fortunei* is considered to be useful in the repair of bones (Chen et al., 2013), and Naringin is an active ingredient of *Drynaria fortunei* which is confirmed to promote osteogenic differentiation in bone marrow-derived mesenchymal stem cells (BMSCs) (Lin et al., 2016). However, whether Naringin can mediate the progression of ONFH remains largely unknown.

MicroRNAs (miRNAs) have been reported to mediate mRNA expression by inhibition of the translation of mRNA (Gerloff et al., 2020). Moreover, miRNAs are known as crucial modulators in ONFH (Wu et al., 2021; Yue et al., 2020). For instance, Huang S et al. found that miR-148a-3p could suppress SMURF1 to prevent the occurrence of ONFH (Huang et al., 2020b). In addition, miR-144-3p could be involved in progression of ONFH (Xiang et al., 2020). Meanwhile, it has been previously proved that miR-26a-CD34-exos protected the GC-induced

* Corresponding author.
E-mail address: zeng3010@163.com (L. Zeng).

https://doi.org/10.1016/j.bonr.2024.101815
Received 14 September 2024; Received in revised form 24 October 2024; Accepted 11 November 2024
Available online 13 November 2024

femoral head via inducing osteogenesis (Zuo et al., 2019). Furthermore, the miRNAs miR-26a/b was reported to target osteogenesis-inhibiting factors to promote osteogenic differentiation in USSCs (Schira-Heinen et al., 2020). In summary, both naringin and miR-26a play significant roles in the regulation of osteogenic differentiation. However, the relation between Naringin and miR-26a in ONFH remains to be explored.

Ski is a homologue of v-ski (oncogene). Its product Ski (called Ski protein in humans and c-Ski protein in animals) is known to be a transcriptional regulator which is participated in the pathophysiological process of various types of cells in many tissues (Lu et al., 2020). Some studies revealed that Ski could play a key role in pathological process. Moreover, Ski mainly depended on BMP-2 and TGF-β signaling to exhibit its function (Ehnert et al., 2012). Meanwhile, Ski has been confirmed to be activated by GC in BMSCs (Zhao et al., 2019). However, the correlation between miR-26a and Ski remains largely unclear. In addition, we found that there are binding sites between miR-26a and Ski by bioinformatics methods. Thus, we speculated Naringin participated in the development of ONFH by regulating miR-26a/Ski axis.

In present study, we aimed to explore the functions of Naringin in AM-treated BMSCs. Our results found that Naringin could strengthen osteogenic potential of BMSCs via mediation of miR-26a/Ski axis. We hope our findings will provide a new agent for ONFH treatment.

2. Material and methods

2.1. Bioinfomatics

Two datasets (GSE89587 and GSE123568) were downloaded from the GEO database (www.ncbi.nlm.nih.gov/geo/) (Clough et al., 2024) to investigate the blood transcriptional characteristics of ONFH. Differential expression analyses were conducted using the limma package in R software. miRNA target genes were predicted using TargetScan database (www.targetscan.org/) (McGeary et al., 2019). GO terms for interested genes were retrieved from the Uniprot database (www.uniprot.org/) (UniProt Consortium, 2023). GO enrichment analysis and corresponding visualizations were performed by an online bioinformatics platform (www.bioinformatics.com.cn) (Tang et al., 2023).

2.2. Cell culture and treatment

Mouse BMSCs and HEK293T cells were purchased from the ATCC (USA) and cultured in DMEM (Gibco, USA) with 10 % FBS (Invitrogen, USA) (37 °C, 5 % CO_2). Naringin was obtained from Sigma-Aldrich (USA). BMSCs were treated with 10 μM, 100 μM or 1000 μM Naringin for 24 h.

To induce adipogenic differentiation in BMSCs, the cells were cultured in an adipogenic medium (AM). This medium consisted of 0.1 μM dexamethasone (Dex, Sigma-Aldrich, USA), 15 % horse serum, and a basal DMEM medium (Lee et al., 2019; Sheng et al., 2007; Justesen et al., 2002). For osteogenic differentiation of BMSCs, BMSCs were treated with osteogenic medium (OM, Sigma-Aldrich, USA) and then cultured.

2.3. Cell transfection

MiR-26a-antago, negative control-antago (NC-antago), miR-26a-ago and NC-ago were obtained from RiboBio (Guangzhou, China). BMSCs were seeded in 6-well plates at a density of 1×10^6 cells/well. And then, BMSCs were transfected with these plasmids by Lipofectamine 2000 (Invitrogen) according to the manufacture's protocol. For Ski overexpression, a lentivirus containing Ski or negative control was purchased from GenePharma (Shanghai, China). Subsequently, BMSCs cells were transfected with LV NC or LV-Ski (Ski overexpression) using Lipofectamine 3000 (Invitrogen).

2.4. Oil Red O Staining

BMSCs were seeded in 24-well plates at a density of 1×10^5 cells/well. The culture medium was removed after BMSCs were induced by AM. Then, BMSCs were washed and fixed with 4 % paraformaldehyde for 30 min. Subsequently, BMSCs were stained with the Oil Red O and incubated for 30 min. After that, solution was discarded and cells were washed and observed by an inverted microscope. Increase of red droplets was considered as the lipid formation in BMSCs.

2.5. Alizarin red staining assay

BMSCs were seeded in 24-well plates at a density of 1×10^5 cells/well. After 7 d of incubation, BMSCs were added with 5 % polyformaldehyde (500 μL) for 10 min and then stained with 200 μL alizarin for 30 min. Then, the calcium nodules were observed by photomicrographs.

2.6. ALP activity assay

BMSCs were seeded in 6-well plates (1×10^6 cells/well) for 24 h. Total protein was extracted from the cells using radioimmunoprecipitation assay (RIPA, Beyotime) buffer and the concentration was quantified by the bicinchoninic acid (BCA, Abcam, USA) assay. ALP activity was measured via using a ALP detection kit according to the manufacturer's instruction. The ALP activity of each sample was normalized against the total protein concentration.

2.7. Reverse transcription quantitative real-time PCR (RT-qPCR)

BMSCs were seeded in 6-well plates (1×10^6 cells/well). Total RNA from BMSCs was obtained with TRIzol reagent (TaKaRa, Tokyo, Japan). Subsequently, reverse transcription kit (TaKaRa) was applied to synthesized cDNA. The following protocol was as follows: 2 min at 94 °C, followed by 40 cycles of 30 s at 94 °C and 45 s at 55 °C. The relative expression of genes was quantified by $2^{-\Delta\Delta Ct}$ method. U6 or β-actin was applied for normalization. Primers were listed as follows: miR-26a 5′-TCCCATTCCCGGAAGCTAGA-3′ (sense), 5′-GAGGCATGAAATCACCCCCA-3′ (anti-sense); Ski 5′-GGCGAAACAAACATGGTGCA-3′ (sense), 5′-CGGCCCAGTGTTCAGACTAC-3′ (anti-sense); β-actin 5′-AGGTCGGAGTCAACGGATTT-3′ (sense), 5′-TGACGGTGCCATGGAATTTG-3′ (anti-sense); U6 5′-CTCGCTTCGGCAGCACA-3′ (sense), 5’-AACGCTTCACGAATTTGCGT-3′ (anti-sense).

2.8. Western blot analysis

BMSCs were seeded in 6-well plates (1×10^6 cells/well). Total protein of BMSCs were extracted by RIPA (Beyotime). BCA Protein Assay Kit (Abcam, USA) was used to test the protein concentration. Equal amounts (20 μg) of protein from each group were separated by sodium dodecyl sulfate polyacrylamide gelelectrophoresis (SDS-PAGE) electrophoresis, and then proteins were transferred onto polyvinylidene fluoride (PVDF) membrane (, Beyotime). After blocked, primary antibodies against Ski (1:2000), Runx2 (1:1000), OCN (1:10000), FABP4 (1:2000), PPAR-γ (1:1000) were incubated at 4 °C overnight and the secondary antibody (1:5000) were used to incubate for 2 h at room temperature. All the antibodies were obtained from Abcam (MA, USA) and then visualized using ECL Western Blot Kit (CWBIO). GAPDH (1:1000) was used for normalization.

2.9. Triglycerides (TG) detection

BMSCs were seeded in 6-well plates (1×10^6 cells/well). BMSCs of different treatment groups were collected and then cell lysed, after centrifugation, the supernatant was collected for TG concentration determination. The content of TG was detected by TG detection kit (MA,

USA). The protocol was in accordance with the previous reference (Tang et al., 2020).

2.10. Bioinformatics analysis and dual luciferase assay

The interaction between miR-26a and Ski was predicted using starBase. Ski fragments with wild-type or mutant miR-26a binding sequences were obtained from GenePharma. The WT and MUT sequences of Ski were transcribed into the pmirGLO luciferase reporter vector (Promega, Madison, Wisconsin, USA) and named Ski-WT and Ski-MUT, respectively. HEK293T cells were seeded in 10 cm^2 dishes (5×10^6 cells/dish). The miR-26a-ago or NC-ago and Ski-WT/MUT was co-transfected into HEK293T cells with Lipofectamine 3000. The luciferase activity was tested by dual luciferase reporter system (Promega).

2.11. Statistical analysis

All data were statistically evaluated using GraphPad Prism 6.0 software. The experiments were conducted at least three replications, and the data were presented as mean ± SD. The comparisons between two groups were analyzed by Student's *t*-test, and the differences between multiple groups were compared by one-way analysis of variance (ANOVA). $P < 0.05$ was considered statistically significant.

3. Results

3.1. miR-26a and Ski were differentially expressed in ONFH and involved in osteogenic/adipogenic differentiation

Utilizing bioinformatics analysis, we identified a significant downregulation of miR-26a (Fig. 1A) and a significant upregulation of Ski (Fig. 1B) in the peripheral blood of patients with ONFH. Through enrichment analysis, it was determined that miR-26a plays a role in regulating the biological process of cell differentiation (Fig. 1C). Following this, an investigation of the Uniprot database for GO terms associated with SKI revealed that SKI is implicated in the negative regulation of osteoblastic differentiation (Fig. 1D). Subsequently, BMSCs were cultured with OM and AM to induce osteogenic and adipogenic differentiation, respectively. As shown in Fig. 1E, OM significantly increased the matrix mineralization in BMSCs. In addition, ALP activity in BMSCs was notably upregulated by OM (Fig. 1F). These data revealed that osteogenic differentiation of BMSCs was significantly promoted by OM. Meanwhile, AM significantly promoted the lipid formation in BMSCs (Fig. 1G), and the content of TG in BMSCs was greatly enhanced by AM (Fig. 1H), suggesting AM notably promoted the adipogenic differentiation of BMSCs. The protein levels of OCN and Runx2 in BMSCs were significantly increased by OM, and AM obviously enhanced the expressions of PPAR-γ and FABP4 in BMSCs (Fig. 1I). We further investigated the expression changes of miR-26a and Ski during osteogenic and adipogenic differentiation of BMSCs. miR-26a level in BMSCs was significantly upregulated by OM, while inhibited by AM (Fig. 1J). OM significantly suppressed Ski expression in BMSCs, while AM exhibited opposite effect (Fig. 1J and K). All these data revealed that miR-26a was upregulated in OM-treated BMSCs, while Ski was downregulated.

3.2. Naringin significantly promoted osteogenic differentiation and inhibited adipogenic differentiation in BMSCs

To detect the effect of Naringin on osteogenic differentiation in BMSCs, alizarin red staining assay was performed. As revealed in Fig. 2A, Naringin significantly enhanced OM-induced increase of matrix mineralization in a dose dependent manner. Consistently, Naringin obviously increased ALP activity in OM-treated BMSCs (Fig. 2B). Naringin reversed AM-induced upregulation of the lipid formation and TG content in BMSCs in a dose-dependent manner (Fig. 2C and D). The protein expressions of OCN and Runx2 in BMSCs were significantly upregulated by OM, which were further enhanced by Naringin (Fig. 2E). AM-induced activation of PPAR-γ and FABP4 in BMSCs was significantly reversed by Naringin (Fig. 2E). Furthermore, the effect of OM or AM on miR-26a expression in BMSCs was obviously rescued by Naringin (Fig. 2F). Taken together, Naringin could promote osteogenic differentiation in BMSCs.

3.3. MiR-26a notably regulated osteogenic and adipogenic differentiation in BMSCs

To investigate the effect of miR-26a on osteogenic and adipogenic differentiation, BMSCs were transfected with miR-26a-ago or antago. As shown in Fig. 3A, miR-26a level in BMSCs was significantly upregulated by miR-26a-ago but decreased by miR-26a-antago. In addition, the data of alizarin red staining assay indicated that miR-26a knockdown reversed OM-induced osteogenic differentiation in BMSCs (Fig. 3B). OM-induced increase of ALP activity was inhibited by miR-26a inhibition (Fig. 3C). The lipid formation in AM-cultured BMSCs was significantly decreased by upregulation of miR-26a (Fig. 3D), and overexpression of miR-26a greatly reversed AM-induced upregulation of TG levels in BMSCs (Fig. 3E). Meanwhile, the protein levels of OCN and Runx2 in BMSCs were upregulated by OM, while this phenomenon was reversed by miR-26a-antago (Fig. 3F). AM-induced increase of PPAR-γ and FABP4 in BMSCs was rescued by miR-26a-ago (Fig. 3F). To sum up, miR-26a could notably regulate osteogenic and adipogenic differentiation in BMSCs.

3.4. Naringin regulated Ski expression in BMSCs via mediation of miR-26a

To detect the effect of Naringin on Ski expression in BMSCs, RT-qPCR was applied. The data suggested Ski level in OM-treated BMSCs was obviously inhibited by Naringin (Fig. 4A). AM-induced upregulation of Ski was significantly inhibited by Naringin (Fig. 4B). Meanwhile, Ski was the potential target of miR-26a (Fig. 4C), and the relative luciferase activity in WT-Ski was decreased by miR-26a-ago (Fig. 4C). Ski level in BMSCs was inhibited by overexpression of miR-26a but increased by knockdown of miR-26a (Fig. 4D and E). Thus, Naringin regulated Ski expression in BMSCs via mediation of miR-26a.

3.5. Naringin regulated osteogenic and adipogenic differentiation in BMSCs via mediation of miR-26a/Ski axis

For the purpose of investigating the efficiency of Ski overexpression, RT-qPCR and Western blotting were used. The results indicated Ski expression level in BMSCs was significantly increased by overexpression of Ski (Fig. 5A and B). In addition, Naringin-induced osteogenic differentiation in OM-treated BMSCs was significantly inhibited by miR-26a inhibition or Ski overexpression (Fig. 5C). Inhibition of miR-26a or overexpression of Ski reversed the promotion effect of Naringin on ALP activity in OM-treated BMSCs (Fig. 5D). Naringin-decreased lipid formation in AM-induced BMSCs was restored by miR-26a knockdown or Ski overexpression (Fig. 5E), and Naringin-induced decrease of TG content in AM-treated BMSCs was partially reversed by miR-26a inhibition or Ski overexpression (Fig. 5F). Moreover, the regulation effect of Naringin on OCN, Runx2, PPAR-γ and FABP4 was significantly rescued by miR-26a-antago or Ski overexpression (Fig. 5G). These data suggesting that Naringin regulated osteogenic and adipogenic differentiation in BMSCs via mediation of miR-26a/Ski axis.

4. Discussion

ONFH is a frequent disease which is caused by GC consumption, alcohol abuse and hip trauma (Sheng et al., 2020). ONFH leads to the dysfunction of BMSCs (Yue et al., 2020; Nonokawa et al., 2020). GC-

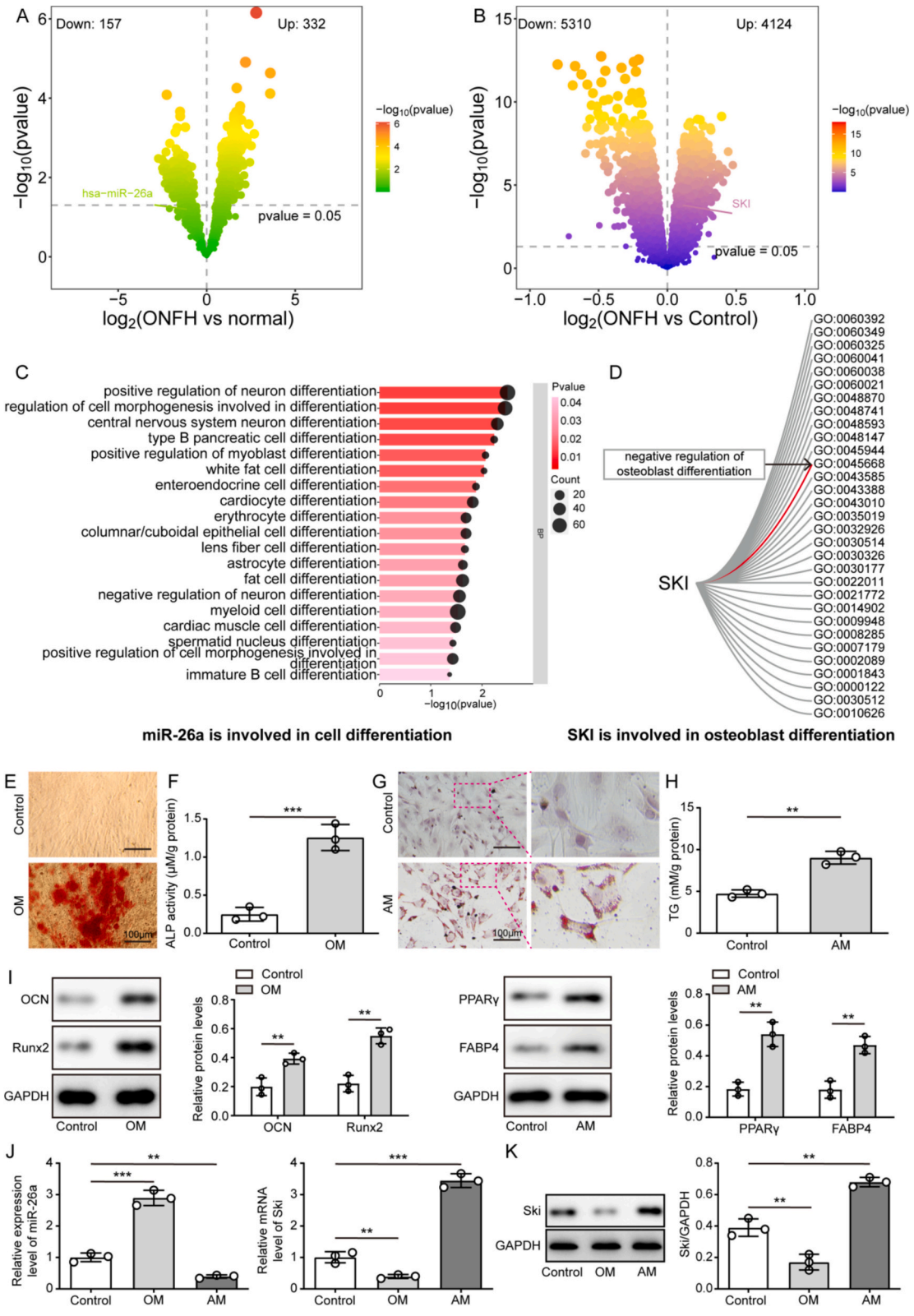

Fig. 1. miR-26a and Ski were differentially expressed in ONFH and involved in osteogenic/adipogenic differentiation. (A) Volcano plot of miRNAs expression in ONFH. (B) Volcano plot of mRNA expression in ONFH. (C) GO analysis for miRNA target genes. (D) SKI-related GO terms. (E) The formation of calcified nodules in BMSCs after treated with OM for 48 h was tested by alizarin red staining. (F) The activity of ALP in BMSCs after treated with OM for 48 h was detected by ALP kit (n = 3, Student's t-test). (G) The lipid formation in BMSCs after treated with AM was tested by oil red O staining. (H) The content of TG in BMSCs after treated with AM was detected by TG detection kit (n = 3, Student's t-test). (I) The protein expressions of OCN, Runx2, PPAR-γ and FABP4 in BMSCs were assessed by Western blotting. GAPDH was applied for normalization (n = 3, Student's t-test). (J) The expression of miR-26a and Ski in BMSCs were tested by RT-qPCR (n = 3, ANOVA). (K) The protein level of Ski in BMSCs was assessed by Western blotting. GAPDH was applied for quantification (n = 3, ANOVA). The boxed border regions were enlarged. Values were presented as means ± SD. Scale bar: 100 μm. $^{**}P < 0.01$, $^{***}P < 0.001$.

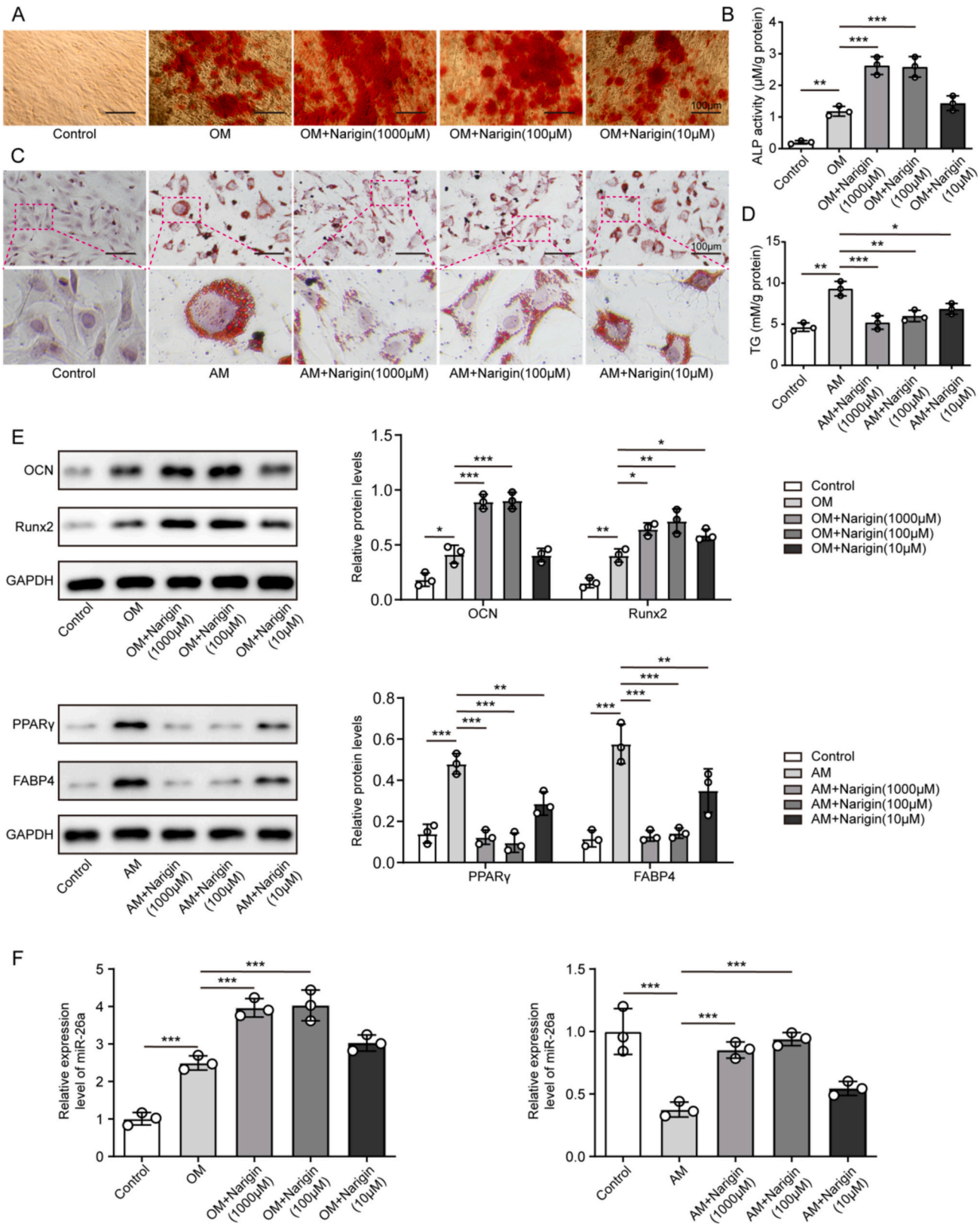

Fig. 2. Naringin significantly promoted osteogenic differentiation and inhibited adipogenic differentiation in BMSCs. BMSCs were treated with OM, and supplemented with 10 μM, 100 μM or 1000 μM Naringin. **(A)** Calcified nodules formation in BMSCs was tested by alizarin red staining. **(B)** The activity of ALP in BMSCs was detected by ALP kit. BMSCs were treated with AM, AM + 10 μM Naringin, AM + 100 μM Naringin or AM + 1000 μM Naringin. **(C)** The lipid formation in BMSCs was tested by oil red O staining. **(D)** The content of TG in BMSCs was detected by TG detection kit. **(E)** The protein expressions of OCN, Runx2, PPAR-γ and FABP4 in BMSCs were assessed by Western blotting. GAPDH was applied for normalization. **(F)** MiR-26a level in BMSCs was tested by RT-qPCR. ($n = 3$, ANOVA). The boxed border regions were enlarged. Values were presented as means ± SD. Scale bar: 100 μm. $^{*}P < 0.05$, $^{**}P < 0.01$, $^{***}P < 0.001$.

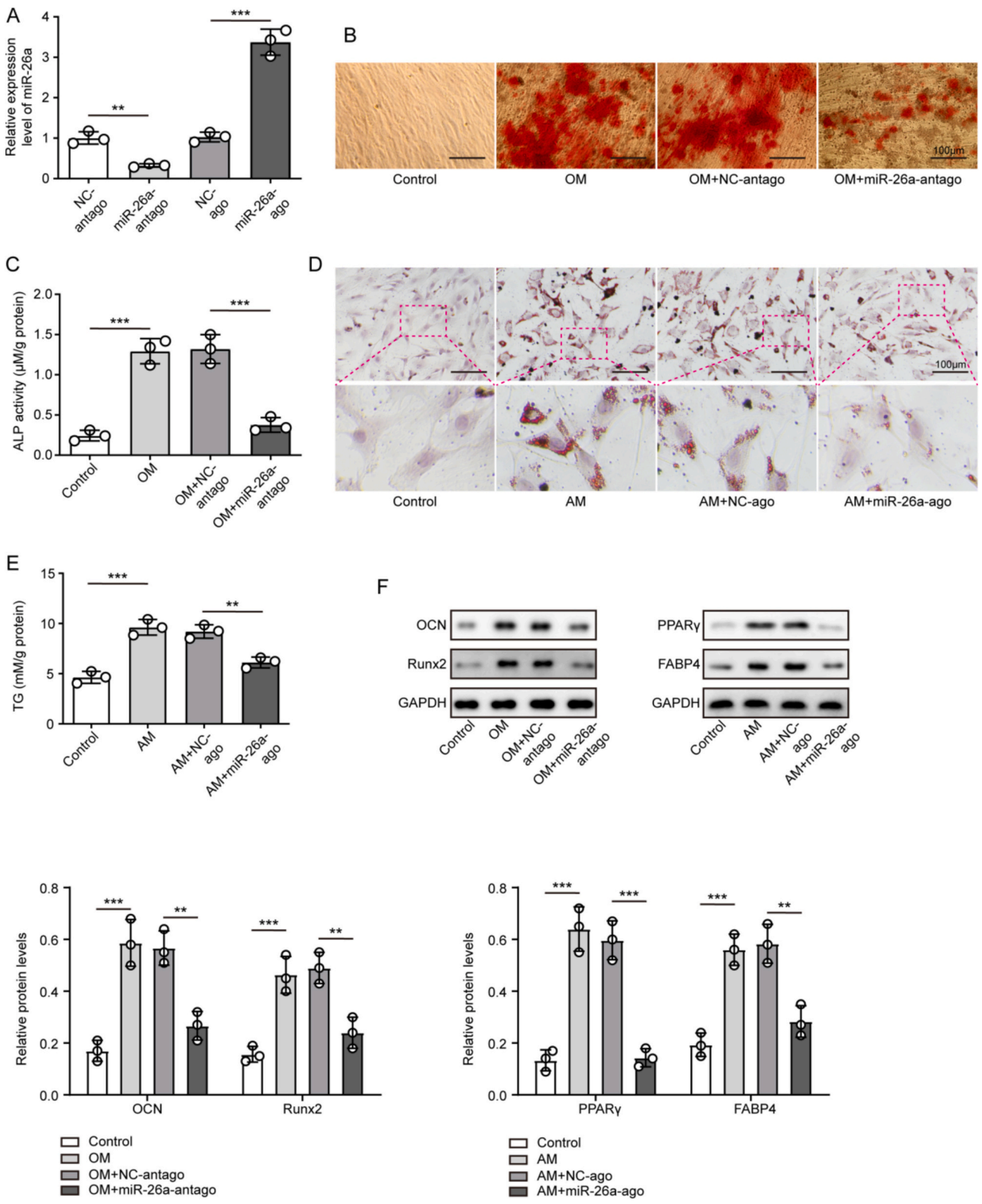

Fig. 3. MiR-26a regulated osteogenic and adipogenic differentiation. **(A)** BMSCs were transfected with miR-26a-ago or antago for 48 h. The expression of miR-26a was tested by RT-qPCR. BMSCs were treated with OM, and then supplemented with NC-antago or miR-26a antago. **(B)** Calcified nodules formation in BMSCs was tested by alizarin red staining. **(C)** The activity of ALP in BMSCs was detected by ALP kit. BMSCs were treated with AM, and then supplemented with NC-ago or miR-26a-ago. **(D)** The lipid formation in BMSCs was tested by oil red O staining. **(E)** The content of TG in BMSCs was detected by TG detection kit. **(F)** The protein expressions of OCN, Runx2, PPAR-γ and FABP4 in BMSCs were assessed by Western blotting. GAPDH was applied for quantification. ($n = 3$, ANOVA). The boxed border regions were enlarged. Values were presented as means ± SD. Scale bar: 100 μm. $^{**}P < 0.01$, $^{***}P < 0.001$.

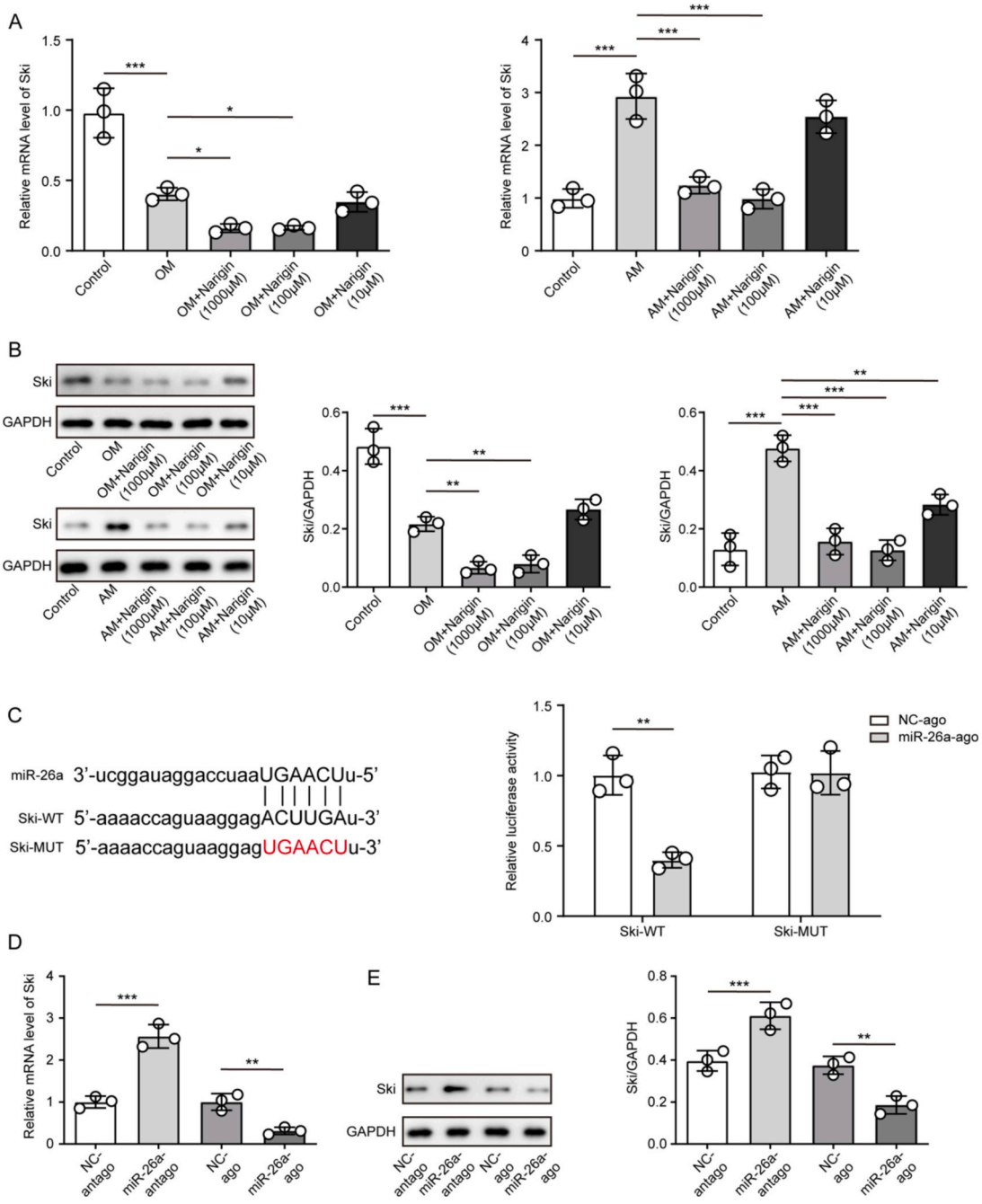

Fig. 4. Naringin regulated Ski expression in BMSCs via mediation of miR-26a. BMSCs were treated with OM/AM, OM/AM + 10 μM Naringin, OM/AM + 100 μM Naringin or OM/AM + 1000 μM Naringin. **(A)** The expression of Ski in BMSCs was detected by RT-qPCR. **(B)** Ski protein level in BMSCs was assessed by Western blotting. GAPDH was applied for normalization. **(C)** Starbase was applied to predict the binding site between miR-26a and Ski. Dual luciferase report assay was applied to test the luciferase activity. BMSCs were treated with miR-26-ago or miR-26a-antago. **(D)** The mRNA level of Ski in BMSCs was detected by RT-qPCR. **(E)** Ski protein level in BMSCs was assessed by Western blotting. GAPDH was applied for quantification. ($n = 3$, ANOVA). The boxed border regions were enlarged. Values were presented as means ± SD. $^{*}P < 0.05$, $^{**}P < 0.01$, $^{***}P < 0.001$.

induced osteonecrosis of the femoral head is the most common type of ONFH, and nearly half of patients with ONFH were induced in China (Duan et al., 2020; Yin et al., 2020). Nowadays, the pathogenesis of ONFH is largely unknown and the main method for treating ONFH is still limited (Wang et al., 2020). It has been reported that the destruction of the balance between osteogenic differentiation and adipogenic differentiation may lead to the occurrence of ONFH (Ma et al., 2020; Kawasaki et al., 2020). In this study, our bioinformatics analysis demonstrated that in the peripheral blood of patients with ONFH, the expression of miR-26a is downregulated, whereas the expression of Ski is upregulated, and then we determined that Naringin could strengthen osteogenic differentiation and suppress adipogenic differentiation through regulation of miR-26a/Ski axis. Our finding firstly explored the impact of Naringin on ONFH, suggesting a new method for ONFH treatment.

It suggested that Naringin could mediate bone metabolism in GC-induced ONFH via regulation of Akt/Bad signaling pathway (Kuang et al., 2019). Meanwhile, Chen et al. found that polydatin could promote the BMSCs osteogenic differentiation through activating the BMP2-Wnt/β-catenin pathway (Chen et al., 2019). Our research was similar to those

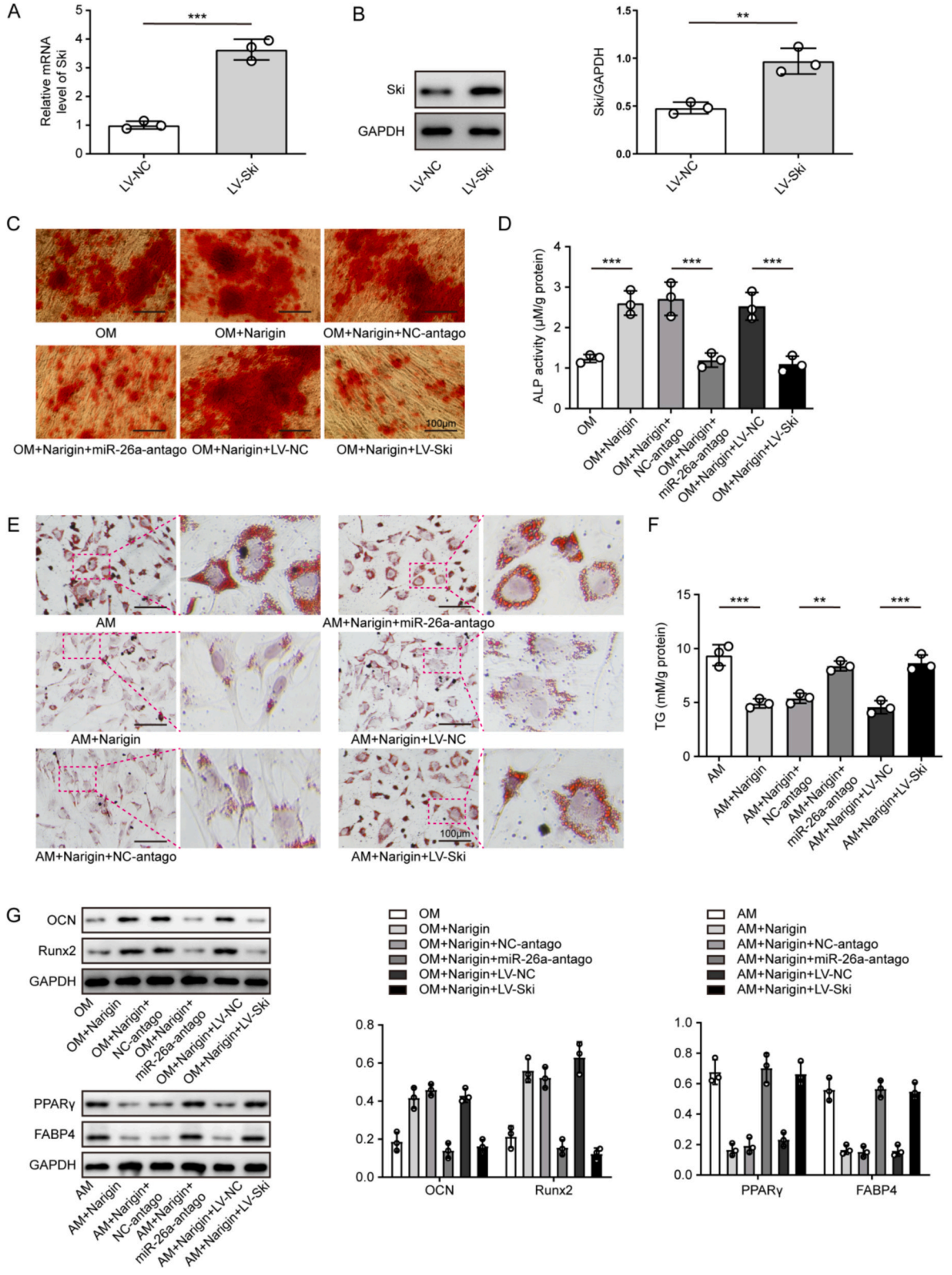

Fig. 5. Naringin regulated osteogenic and adipogenic differentiation via mediation of miR-26a/Ski axis. **(A)** Ski expression in BMSCs after Ski overexpression was detected by RT-qPCR. ($n = 3$, Student's *t*-test) **(B)** Ski protein level in BMSCs after Ski overexpression was assessed by Western blotting. GAPDH was applied for normalization. (n = 3, Student's t-test). BMSCs were treated with OM and miR-26a-antago or Ski overexpression. **(C)** Calcified nodules formation in BMSCs was tested by alizarin red staining. **(D)** The activity of ALP in BMSCs was detected by ALP kit. (n = 3, ANOVA). BMSCs were treated with AM and miR-26a-antago or Ski overexpression. **(E)** The lipid formation was tested by oil red O staining. **(F)** The content of TG in BMSCs was detected by TG detection kit. (n = 3, ANOVA). **(G)** The protein expressions of OCN, Runx2, PPAR-γ and FABP4 in BMSCs were assessed by Western blotting. GAPDH was applied for quantification. (n = 3, ANOVA). The boxed border regions were enlarged. Values were presented as means ± SD. $^{**}P < 0.01$, $^{***}P < 0.001$.

previous study, we found that Naringin could promote osteogenic differentiation and inhibit adipogenic differentiation to suppress the progression of ONFH in vitro. The osteogenic effects of Naringin are multifaceted. In this study, we observed that different concentrations of naringin demonstrated varying levels of osteogenic activity, with more pronounced effects at higher concentrations. Runx2 is a well-established transcription factor that promotes osteogenic differentiation (Kim et al., 2022), and in this study, we used Runx2 as a biomarker for osteogenic differentiation. Our findings suggested that cells treated with various concentrations of naringin displayed significantly different levels of Alizarin red staining. However, no significant differences were observed between the 1000 μM and 100 μM Naringin groups in the WB analysis of Runx2. The observed discrepancy between Alizarin red staining and Runx2 Western blot results could be attributed to the complex mechanisms through which Naringin operates. Furthermore, the lack of Runx2 upregulation in the 1000 μM Naringin group compared to the 100 μM Naringin group may be due to the potential saturation of its pharmacological effects in the presenting condition. Herein, our research supplemented the mechanism by which Naringin modulated the ONFH progression. And Naringin could function as a key regulator in bone metabolism, osteogenic differentiation and adipogenic differentiation.

MiRNAs are known to be participated in BMSCs osteogenesis and adipogenesis. For instance, Cao Y et al. indicated that miR-224-5p could regulate osteogenic and adipogenic differentiation (Cao et al., 2021); Wu F et al. revealed that miR-155-5p could promote proliferation and differentiation of BMSC through targeting GSK3β (Wu et al., 2021); Skarn M et al. proposed that miRNA-155, miRNA-221, and miRNA-222 play a critical role in the adipogenic differentiation of hMSCs (Skårn et al., 2012). In the current research, we found miR-26a could act as an important mediator in differentiation of osteogenesis and adipogenesis. Together, miRNAs are integral elements of the intricate regulatory network that governs cellular differentiation into osteogenic and adipogenic lineages. Our results showed that miR-26a promoted osteogenic differentiation of BMSC by increasing the expression of osteogenic genes including OCN and RUNX2. Li G et al. found that upregulation of miR-26a could protect ONFH via downregulation of enhancer of zeste homologue 2 (EZH2) (Li et al., 2020). Our study was consistent to this research, suggesting miR-26a was activated during BMSCs osteogenic differentiation, and could promote osteogenic differentiation as well as inhibit adipogenic differentiation.

MiRNAs can regulate protein expression by binding to mRNA 3′- UTR (Fabian et al., 2010). In present study, Ski was found to be the target mRNA of miR-26a, and Naringin promoted osteogenic differentiation of BMSCs by mediating miR-26a/Ski axis. Previous studies found that glucocorticoid could increase the level of Ski in ONFH, and it could promote the adipogenesis of BMSCs (Zhao et al., 2019; Yang et al., 2012). Consistently, our research indicated that Ski could reverse the regulation effect of miR-26a on BMSC function. Simultaneously, EZH2, recognized as a gene associated with bone metabolism (Xu et al., 2020; Zerif et al., 2020), has been validated to mediate the osteogenic effects of miR-26a (Li et al., 2020). This suggests a shared involvement of EZH2 and Ski in the formation of the regulatory network of miRNA-26a during osteogenic differentiation. The identification of target genes such as EZH2 and Ski provides novel insights into the comprehensive understanding of miR-26a's role as a regulator in osteogenesis, thereby facilitating the clinical translation of therapeutic targets for ONFH. In addition, it reported that expressions of Ski, PPAR-γ and FABP4 were upregulated in GC-induced ONFH (Zhao et al., 2019). Our research showed that Ski expression decreased during osteogenic differentiation and overexpression of Ski could reverse the promotion of Naringin on bone formation of BMSC, confirming that Ski might be the key biomarkers in ONFH.

Our study, while providing valuable insights through in vitro cell-based experiments, is limited by the absence of in vivo validation. The use of animal models would offer a more comprehensive understanding of the miR-26a's effects on osteogenesis and potential therapeutic effects of our findings in a whole-organism context. In conclusion, Naringin could strengthen osteogenic potential in BMSCs via mediation of miR-26a/ski axis. Thereby, Naringin has the potential to become a promising therapeutic agent for ONFH treatment.

Abbreviations

Dex	dexamethasone
OM	osteogenic medium
ONFH	osteonecrosis of the femoral head
BMSCs	bone marrow-derived mesenchymal stem cells
MiRNA	microRNA
OCN	osteocalcin
Runx2	Runt-related transcription factor 2
FABP4	fatty acid binding protein 4
PPARγ	peroxisome proliferator-activated receptor gamma
TG	triglyceride

CRediT authorship contribution statement

Jiawei Zou: Writing – original draft, Visualization, Conceptualization. **Longze Zhou:** Methodology, Data curation. **Guoqiang Liu:** Methodology. **Ying Zhang:** Data curation. **Lingguo Zeng:** Writing – review & editing, Supervision, Methodology, Conceptualization.

Declaration of competing interest

We wish to confirm that there are no known conflicts of interest associated with this publication and there has been no significant financial support for this work that could have influenced its outcome. We confirm that the manuscript has been read and approved by all named authors and that there are no other persons who satisfied the criteria for authorship but are not listed. We further confirm that the order of authors listed in the manuscript has been approved by all of us.

Acknowledgement

Not applicable.

Data availability

Data will be made available on request.

References

Cao, Y., Jiang, C., Wang, X., Wang, H., Yan, Z., Yuan, H., 2021. Reciprocal effect of microRNA-224 on osteogenesis and adipogenesis in steroid-induced osteonecrosis of the femoral head. Bone 115844.

Chen, K.Y., Dong, G.C., Hsu, C.Y., Chen, Y.S., Yao, C.H., 2013. Autologous bone marrow stromal cells loaded onto porous gelatin scaffolds containing Drynaria fortunei extract for bone repair. J. Biomed. Mater. Res. A 101 (4), 954–962.

Chen, X.J., Shen, Y.S., He, M.C., Yang, F., Yang, P., Pang, F.X., et al., 2019. Polydatin promotes the osteogenic differentiation of human bone mesenchymal stem cells by activating the BMP2-Wnt/beta-catenin signaling pathway. Biomed. Pharmacother. 112, 108746.

Clough, E., Barrett, T., Wilhite, S.E., Ledoux, P., Evangelista, C., Kim, I.F., et al., 2024. NCBI GEO: archive for gene expression and epigenomics data sets: 23-year update. Nucleic Acids Res. 52 (D1), D138–D144.

Duan, L., Zuo, J., Zhang, F., Li, B., Xu, Z., Zhang, H., et al., 2020. Magnetic targeting of HU-MSCs in the treatment of glucocorticoid-associated osteonecrosis of the femoral head through Akt/Bcl2/bad/caspase-3 pathway. Int. J. Nanomedicine 15, 3605–3620.

Ehnert, S., Zhao, J., Pscherer, S., Freude, T., Dooley, S., Kolk, A., et al., 2012. Transforming growth factor beta1 inhibits bone morphogenic protein (BMP)-2 and BMP-7 signaling via upregulation of ski-related novel protein N (SnoN): possible mechanism for the failure of BMP therapy? BMC Med. 10, 101.

Fabian, M.R., Sonenberg, N., Filipowicz, W., 2010. Regulation of mRNA translation and stability by microRNAs. Annu. Rev. Biochem. 79, 351–379.

Gerloff, D., Sunderkotter, C., Wohlrab, J., 2020. Importance of microRNAs in skin oncogenesis and their suitability as agents and targets for topical therapy. Skin Pharmacol. Physiol. 1-10.

Guillemet, L., Jamme, M., Bougouin, W., Geri, G., Deye, N., Vivien, B., et al., 2020. Effects of early high-dose erythropoietin on acute kidney injury following cardiac arrest: exploratory post hoc analyses from an open-label randomized trial. Clin. Kidney J. 13 (3), 413–420.

Huang, S., Li, Y., Wu, P., Xiao, Y., Duan, N., Quan, J., et al., 2020b. microRNA-148a-3p in extracellular vesicles derived from bone marrow mesenchymal stem cells suppresses SMURF1 to prevent osteonecrosis of femoral head. J. Cell. Mol. Med. 24 (19), 11512–11523.

Huang, Z.Q., Fu, F.Y., Li, W.L., Tan, B., He, H.J., Liu, W.G., et al., 2020a. Current treatment modalities for osteonecrosis of femoral head in mainland China: a cross-sectional study. Orthop. Surg. 12 (6), 1776–1783.

Justesen, J., Stenderup, K., Eriksen, E.F., Kassem, M., 2002. Maintenance of osteoblastic and adipocytic differentiation potential with age and osteoporosis in human marrow stromal cell cultures. Calcif. Tissue Int. 71 (1), 36–44.

Kawasaki, S., Inagaki, Y., Akahane, M., Furukawa, A., Shigematsu, H., Tanaka, Y., 2020. In vitro osteogenesis of rat bone marrow mesenchymal cells on PEEK disks with heat-fixed apatite by CO2 laser bonding. BMC Musculoskelet. Disord. 21 (1), 692.

Kim, H.J., Cho, H.B., Lee, S., Lyu, J., Kim, H.R., Lee, S., et al., 2022. Strategies for accelerating osteogenesis through nanoparticle-based DNA/mitochondrial damage repair. Theranostics 12 (14), 6409–6421.

Kim, S.C., Lim, Y.W., Jo, W.L., Park, S.B., Kim, Y.S., Kwon, S.Y., 2020. Long-term results of Total hip arthroplasty in young patients with osteonecrosis after allogeneic bone marrow transplantation for hematological disease: a multicenter, propensity-matched cohort study with a mean 11-year follow-up. J. Arthroplasty 36 (3), 1049–1054.

Kuang, M.J., Zhang, W.H., He, W.W., Sun, L., Ma, J.X., Wang, D., et al., 2019. Naringin regulates bone metabolism in glucocorticoid-induced osteonecrosis of the femoral head via the Akt/bad signal cascades. Chem. Biol. Interact. 304, 97–105.

Lee, H.P., Stowers, R., Chaudhuri, O., 2019. Volume expansion and TRPV4 activation regulate stem cell fate in three-dimensional microenvironments. Nat. Commun. 10 (1), 529.

Li, G., Liu, H., Zhang, X., Liu, X., Zhang, G., Liu, Q., 2020. The protective effects of microRNA-26a in steroid-induced osteonecrosis of the femoral head by repressing EZH2. Cell Cycle 19 (5), 551–566.

Lin, F.X., Du, S.X., Liu, D.Z., Hu, Q.X., Yu, G.Y., Wu, C.C., et al., 2016. Naringin promotes osteogenic differentiation of bone marrow stromal cells by up-regulating Foxc2 expression via the IHH signaling pathway. Am. J. Transl. Res. 8 (11), 5098–5107.

Lu, J., Wu, X., Wang, L., Li, T., Sun, L., 2020. Long noncoding RNA LINC00467 facilitates the progression of acute myeloid leukemia by targeting the miR-339/SKI pathway. Leuk. Lymphoma 1-10.

Ma, X., Chen, J., Liu, J., Xu, B., Liang, X., Yang, X., et al., 2020. IL-8/CXCR2 mediates tropism of human bone marrow-derived mesenchymal stem cells toward CD133(+) /CD44(+) Colon cancer stem cells. J. Cell. Physiol. 236 (4), 3114–3128.

Mao, L., Jiang, P., Lei, X., Ni, C., Zhang, Y., Zhang, B., et al., 2020. Efficacy and safety of stem cell therapy for the early-stage osteonecrosis of femoral head: a systematic review and meta-analysis of randomized controlled trials. Stem Cell Res Ther. 11 (1), 445.

McGeary, S.E., Lin, K.S., Shi, C.Y., Pham, T.M., Bisaria, N., Kelley, G.M., et al., 2019. The biochemical basis of microRNA targeting efficacy. Science 366(6472):eaav1741.

Nonokawa, M., Shimizu, T., Yoshinari, M., Hashimoto, Y., Nakamura, Y., Takahashi, D., et al., 2020. Association of Neutrophil Extracellular Traps with the development of idiopathic osteonecrosis of the femoral head. Am. J. Pathol. 190 (11), 2282–2289.

Schira-Heinen, J., Czapla, A., Hendricks, M., Kloetgen, A., Wruck, W., Adjaye, J., et al., 2020. Functional omics analyses reveal only minor effects of microRNAs on human somatic stem cell differentiation. Sci. Rep. 10 (1), 3284.

Sheng, H., Lao, Y., Zhang, S., Ding, W., Lu, D., Xu, B., 2020. Combined pharmacotherapy with alendronate and Desferoxamine regulate the bone resorption and bone regeneration for preventing glucocorticoids-induced osteonecrosis of the femoral head. Biomed. Res. Int. 2020, 3120458.

Sheng, H.H., Zhang, G.G., Cheung, W.H., Chan, C.W., Wang, Y.X., Lee, K.M., et al., 2007. Elevated adipogenesis of marrow mesenchymal stem cells during early steroid-associated osteonecrosis development. J. Orthop. Surg. Res. 2, 15.

Skårn, M., Namløs, H.M., Noordhuis, P., Wang, M.Y., Meza-Zepeda, L.A., Myklebost, O., 2012. Adipocyte differentiation of human bone marrow-derived stromal cells is modulated by microRNA-155, microRNA-221, and microRNA-222. Stem Cells Dev. 21 (6), 873–883.

Tang, D., Chen, M., Huang, X., Zhang, G., Zeng, L., Zhang, G., et al., 2023. SRplot: a free online platform for data visualization and graphing. PloS One 18 (11), e0294236.

Tang, S., Shi, Z., Qiao, X., Zhuang, Z., Ding, Y., Wu, Y., et al., 2020. Carya cathayensis leaf extract attenuates ectopic fat deposition in liver, abdomen and aortic arch in ovariectomized rats fed a high-fat diet. Phytomedicine 82, 153447.

UniProt Consortium, 2023. UniProt: the universal protein knowledgebase in 2023. Nucleic Acids Res. 51 (D1), D523–D531.

Wang, X.Y., Gong, L.J., Huang, J.M., Jiang, C., Yan, Z.Q., 2020. Pinocembrin alleviates glucocorticoid-induced apoptosis by activating autophagy via suppressing the PI3K/Akt/mTOR pathway in osteocytes. Eur. J. Pharmacol. 880, 173212.

Wu, F., Huang, W., Yang, Y., Liu, F., Chen, J., Wang, G., et al., 2021. miR-155-5p regulates mesenchymal stem cell osteogenesis and proliferation by targeting GSK3B in steroid-associated osteonecrosis. Cell Biol. Int. 45 (1), 83–91.

Xiang, S., Li, Z., Weng, X., 2020. Changed cellular functions and aberrantly expressed miRNAs and circRNAs in bone marrow stem cells in osteonecrosis of the femoral head. Int. J. Mol. Med. 45 (3), 805–815.

Xu, B.P., Yao, M., Tian, Z.R., Zhou, L.Y., Yang, L., Li, Z.J., et al., 2019b. Study on efficacy and safety of Tong-luo Qu-tong plaster treatment for knee osteoarthritis: study protocol for a randomized, double-blind, parallel positive controlled, multi-center clinical trial. Trials 20 (1), 377.

Xu, Y., Liu, X., Li, H., Liu, H., Pan, Z., Chen, G., 2019a. Brain neural effects of the 'tonifying kidney and benefiting marrow' method in the treatment of osteoporosis. J. Tradit. Chin. Med. 39 (6), 902–909.

Xu, Y., Liu, N., Wei, Y., Zhou, D., Lin, R., Wang, X., et al., 2020. Anticancer effects of miR-124 delivered by BM-MSC derived exosomes on cell proliferation, epithelial mesenchymal transition, and chemotherapy sensitivity of pancreatic cancer cells. Aging (Albany NY) 12 (19), 19660–19676.

Yang, L., Chang, N., Liu, X., Han, Z., Zhu, T., Li, C., et al., 2012. Bone marrow-derived mesenchymal stem cells differentiate to hepatic myofibroblasts by transforming growth factor-beta1 via sphingosine kinase/sphingosine 1-phosphate (S1P)/S1P receptor axis. Am. J. Pathol. 181 (1), 85–97.

Yang, R.C., Chang, C.C., Sheen, J.M., Wu, H.T., Pang, J.H., Huang, S.T., 2014. Davallia bilabiata inhibits TNF-alpha-induced adhesion molecules and chemokines by suppressing IKK/NF-kappa B pathway in vascular endothelial cells. Am. J. Chin. Med. 42 (6), 1411–1429.

Yin, B.H., Chen, H.C., Zhang, W., Li, T.Z., Gao, Q.M., Liu, J.W., 2020. Effects of hypoxia environment on osteonecrosis of the femoral head in Sprague-Dawley rats. J. Bone Miner. Metab. 38 (6), 780–793.

Yue, J., Yu, H., Liu, P., Wen, P., Zhang, H., Guo, W., et al., 2020. Preliminary study of icariin indicating prevention of steroid-induced osteonecrosis of femoral head by regulating abnormal expression of miRNA-335 and protecting the functions of bone microvascular endothelial cells in rats. Gene 766, 145128.

Zerif, E., Khan, F.U., Raki, A.A., Lullier, V., Gris, D., Dupuis, G., et al., 2020. Elucidating the role of Ezh2 in Tolerogenic function of NOD bone marrow-derived dendritic cells expressing constitutively active Stat5b. Int. J. Mol. Sci. 21 (18).

Zhao, X., Wei, Z., Li, D., Yang, Z., Tian, M., Kang, P., 2019. Glucocorticoid enhanced the expression of ski in osteonecrosis of femoral head: the effect on Adipogenesis of rabbit BMSCs. Calcif. Tissue Int. 105 (5), 506–517.

Zuo, R., Kong, L., Wang, M., Wang, W., Xu, J., Chai, Y., et al., 2019. Exosomes derived from human CD34(+) stem cells transfected with miR-26a prevent glucocorticoid-induced osteonecrosis of the femoral head by promoting angiogenesis and osteogenesis. Stem Cell Res Ther 10 (1), 321.